NUMERICAL ANALYSIS OF MICRO-FRACTURE MAPS IN NOTCHED SPECIMENS

J. Toribio* and E. Vasseur†

A combined approach to integrate experimental and numerical methods in structural integrity is proposed. Fracture tests were conducted on axi-symmetric notched samples of high-strength steel. Fractographic analysis showed the microscopic topographies after failure and allowed the assembly of micro-fracture maps (MFM) covering the whole fracture surface and containing information on the micromechanisms of fracture in the material. Finite element computations gave the distribution of macroscopic variables at the fracture instant in the area covered by the MFM, to correlate the distribution of continuum mechanics variables with the different topographies included in the MFM.

INTRODUCTION

The fundamental ideas in the field of micromechanical aspects of fracture have been formulated in past decades (cf. Mc Clintock (1), Rice and Tracey (2), Gurson (3)). In recent years, extensive work has been devoted to ductile failure theories on the basis of nucleation and growth of holes (cf. Goods and Brown (4), Le Roy et al (5)), so it is well established that the growth rate of micro-voids is an increasing function of the stress triaxiality.

This contribution offers a combined fractographic and numerical analysis of the fracture surface of eutectoid pearlitic steel in the form of notched samples of different geometries. Analysis is focussed on the development of micro-fracture maps (MFM) from testing results and further interpretation by using adequate computational methods for stress-strain analysis at the failure instant.

* Departamento de Ciencia de Materiales, Universidad de La Coruña
ETSI Caminos, Campus de Elviña, 15192 La Coruña, Spain
† Centre des Matériaux, Ecole des Mines de Paris
B.P. 87, 91003 Evry Cédex, France

EXPERIMENTAL PROGRAMME

A high strength pearlitic steel was used, whose chemical composition and mechanical properties are respectively given in Tables 1 and 2. It presents a coarse pearlitic microstructure, with a pearlite interlamellar spacing of 0.3 μm, an average size of the cleavage facet of 75 μm, and an average pearlite colony size of about 15 μm.

TABLE 1– Chemical composition of the steel (wt %)

C	Mn	Si	P	S	Cr	Ni	Mo
0.85	0.60	0.26	0.010	0.030	0.02	0.02	0.001

TABLE 2– Mechanical properties of the steel

Young's Modulus	Yield Strength	UTS	Elong. at UTS	Ramberg-Osgood parameters	
(GPa)	(MPa)	(MPa)	(%)	P (MPa)	n
199	600	1151	6.1	2100	4.9

P,n: Ramberg-Osgood Parameters $\varepsilon = \sigma/E + (\sigma/P)^n$

Fracture tests under tension loading were performed on axisymmetric notched specimens with a circumferentially-shaped notch (Fig. 1). Four notch geometries were used with very different depths and radii, in order to achieve very different stress states in the vicinity of the notch tip and thus very distinct *constraint* situations (different level of *triaxiality*), thus allowing an analysis of the influence of these important parameters on the micromechanical fracture processes.

Macroscopic results of the fracture tests may be summarized as follows. Geometries A, B and C presented a macroscopically brittle fracture behaviour; geometry D is the only one that presented a macroscopically ductile behaviour with clear decrease in load. These macroscopically brittle or ductile behaviours are defined on the basis of the load-displacement curve for the fracture tests: brittle if there is no decrease in load and ductile when the curve presents a significant load decrease after the point of maximum load.

MICRO-FRACTURE MAPS

SEM fractographic analysis showed that the fracture always initiates by *micro-void coalescence* (MVC) in a *fibrous* or *dimpled* region and propagates in unstable manner by *cleavage-like* (C) in geometries A, B and C, or in stable manner by MVC followed by shear lip (L) in geometry D. The macroscopic fracture mode is peripheral and plane in the first case and central with *cup and cone* shape in the second. Cleavage is oriented in geometries A and C (single initiation point) and randomly oriented in geometry B (multiple initiation locations).

To allow a detailed analysis of the fracture surface, MFM were assembled covering the whole fracture surface of all geometries and containing information on the micromechanisms of fracture in the material. Fig. 2 offers the MFM of geometry B. It shows an external MVC ring (initiation area) with three predominant locations (more or less at 120 degrees) from which three cleavage fronts propagate. As a consequence of this placement, final fracture by shear-lip is found in internal regions located also in three predominant orientations.

NUMERICAL ANALYSIS AND DISCUSSION

To find the distribution of macroscopic continuum mechanics variables at the fracture instant, the finite element method (FEM) with an elastic-plastic code was applied. Computer results showed that the *triaxiality* (i.e., the ratio of the hydrostatic to the equivalent stress) was the variable governing the microscopical fracture process. Fig. 3 shows the triaxiality distribution in all samples at the fracture instant, as well as the triaxiality factor (maximum in the sample).

Previous analyses by Toribio et al (6) were based in an *average* estimation of the MVC depth over the whole external ring (obviously below the maximum MVC depth) and they showed the existence of a *characteristic triaxiality level* below which the fracture is MVC and above which it is cleavage-like. On the basis of the measurement of the *maximum* MVC depth in the sample, the conclusion does not seem so clear. However, there is a decreasing relation between this maximum MVC depth and the *triaxiality factor* of the geometry, except in geometry B in which fracture process initiates at the boundary and maximum triaxiality is achieved at the center of the sample. This is consistent with the existence of a critical size of micro-void which is a decreasing function of the triaxiality (Pineau (7), Beremin (8)). Once the critical size of void is reached, unstable fracture takes place by cleavage. From a *local* point of view, it is well known that the rate of growth of holes (micro-voids) is an increasing function of the stress triaxiality at the considered point (2). From a *global* point of view, the level of triaxiality —or global constraint— in the sample controls the initiation of unstable fracture by cleavage. The greater the global constraint (triaxiality factor), the lower the depth of the MVC region. These explanations are also consistent with recent studies on fracture of prismatic notched samples of pearlitic steel (Toribio et al (9)).

CONCLUSIONS

The MFM can be interpreted by numerical analysis, and the triaxiality turns out to be the variable governing the extension of the MVC region where fracture initiates in notched samples of pearlitic steel. Although the void growth *rate* increases as the *local* triaxiality does, from the *global* point of view the MVC zone is a decreasing function of the triaxiality factor, since the *critical* void growth rate decreases as the triaxiality increases. A characteristic value of triaxiality seems to exist below which fracture is MVC and above which it is cleavage-like. Limit situations such as smooth sample (minimum triaxiality) and cracked one (maximum triaxiality) are included in this criterion, since the smooth sample breaks y MVC, whereas the cracked one breaks by cleavage.

ACKNOWLEDGEMENTS

This work was funded by the Spanish DGICYT (Grant UE94-001) and Xunta de Galicia (Grants XUGA 11801A93 and XUGA 11801B95). In addition, authors are also indebted to the Commision of the European Communities (*Human Capital and Mobility* Programme-Grant ERBCHBICT930848) for supporting the stay of Dr. E. Vasseur as a Visiting Researcher at the University of La Coruña (Spain).

REFERENCES

(1) Mc Clintock, F.A., J. Applied Mechanics, Vol. 35, 1968, pp. 363-371.

(2) Rice, J.R. and Tracey, D.M., J. Mech. Phys. Solids, Vol. 17, 1969, pp. 201-217.

(3) Gurson, A.L., J. Engng. Mater. Tech., Vol. 99, 1977, pp. 2-14.

(4) Goods, S.H. and Brown, L.M., Acta metall., Vol. 27, 1979, pp. 1-15.

(5) Le Roy, G., Embury, J.D., Edward, G. and Ashby, M.F., Acta Metall., Vol. 29, 1981, pp. 1509-1522.

(6) Toribio, J., Lancha, A.M. and Elices, M., Mater. Sci. Engng., Vol. A145, 1991, pp. 167-177.

(7) Pineau, A., "Advances in Fracture Research (ICF5)". Edited by D. Francois, Pergamon, Oxford, 1981, pp. 553-577.

(8) Beremin, F.M., "Advances in Fracture Research (ICF5)".Edited by D. Francois, Pergamon, Oxford, 1981, pp. 809-816.

(9) Toribio, J., Vasseur, E. and Justo, E.R., Anal. Mec. Fract., Vol. 12, 1995, pp. 185-190.

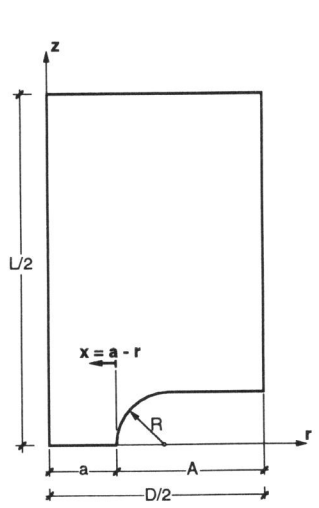

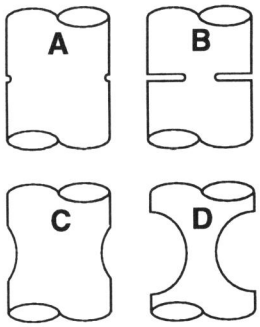

Sample	R/D	A/D
A	0.03	0.10
B	0.05	0.39
C	0.36	0.10
D	0.40	0.39

Figure 1 Notched geometries

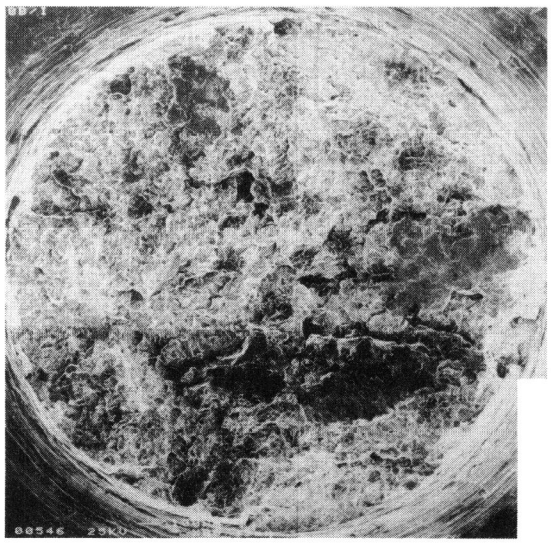

Figure 2 Micro-fracture map (MFM) of geometry B.

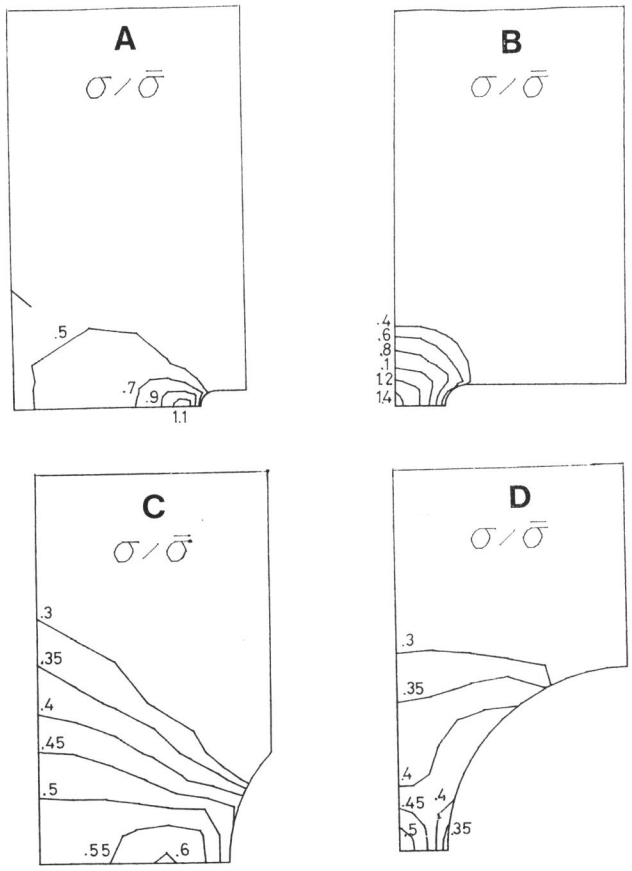

Sample	T = Sup ($\sigma/\bar{\sigma}$)	
	Elastic	Fracture
A	0.9	1.1
B	1.4	1.4
C	0.5	0.6
D	0.4	0.5

Figure 3 Triaxiality distribution in the samples at the fracture instant, and triaxiality factor (maximum) in the elastic and fracture regimes.